Rare-Earth Gallium Antimonides $La_{13}Ga_8Sb_{21}$ and $RE_{12}Ga_4Sb_{23}$ (RE = La−Nd, Sm): Linking Sb Ribbons by Ga_6-Rings or Ga_2-Pairs

Allison M. Mills and Arthur Mar*

Department of Chemistry, University of Alberta, Edmonton, Alberta, Canada T6G 2G2

Received May 16, 2000

The ternary rare-earth gallium antimonides $La_{13}Ga_8Sb_{21}$ and $RE_{12}Ga_4Sb_{23}$ (RE = La−Nd, Sm) have been synthesized through reaction of the elements. The structures of $La_{13}Ga_8Sb_{21}$ (hexagonal, space group D^1_{6h}-$P6/mmm$, $Z = 1$, $a = 17.657(2)$ Å, $c = 4.3378(7)$ Å) and $Pr_{12}Ga_4Sb_{23}$ (orthorhombic, space group D^{25}_{2h}-$Immm$, $Z = 2$, $a = 4.2612(3)$ Å, $b = 19.4070(13)$ Å, $c = 26.3972(18)$ Å) have been determined by single-crystal X-ray diffraction. Both structures contain groupings of RE_6 trigonal prisms that extend as columns through sharing of the triangular faces. Isolated trigonal planar $GaSb_3$ units result from centering adjacent trigonal prisms by Ga or Sb atoms. Channels outlined by Sb square ribbons linked through Ga−Ga bonding enclose the triangular assemblies of trigonal prisms. The Ga−Ga bonding is manifested as Ga_6-rings in $La_{13}Ga_8Sb_{21}$ but as Ga_2-pairs in $Pr_{12}Ga_4Sb_{23}$. Structural relationships are described between $La_{13}Ga_8Sb_{21}$ and $Ba_{0.8}Hf_{12}As_{17.7}$, and between $Pr_{12}Ga_4Sb_{23}$ and La_6MnSb_{15}.

Introduction

Solid-state compounds of the post-transition metals and metalloids display a remarkable variety of structures that challenge our assumptions on what kinds of bonding are possible. There now exist many ternary compounds $M_xA_yB_z$ containing an electropositive component M (alkali or alkaline-earth metal) and two main-group elements A and B, classified as Zintl phases, in which an electron-precise formulation is possible and bonding is readily understood in terms of the fulfilment of closed-shell configurations through the formation, if necessary, of homoatomic bonds.[1] In general, it is the more electronegative main-group element B that participates in such additional homoatomic bonding. Thus, for instance, in the overwhelming majority of ternary alkali or alkaline-earth metal gallium antimonides, $M_xGa_ySb_z$, the less electronegative Ga atoms complete their octets almost invariably through heteroatomic Ga−Sb bonds, while the more electronegative Sb atoms do so through the presence of lone pairs or through the formation of homoatomic Sb−Sb bonds.[2] As a result, the most common building blocks in these compounds are tetrahedral $GaSb_4$ and trigonal planar $GaSb_3$ units. These tetrahedra or trigonal planes may occur as isolated anions, or may be condensed via corner-sharing or through Sb−Sb bonds into oligomers, polymeric chains, or more extended networks. Standing in stark contrast, then, is the case of $Na_2Ga_3Sb_3$, the only compound in this system where Ga−Ga bonding is also present.[2a]

Substitution of the alkali or alkaline-earth metal by a rare-earth metal kicks up the complexity of the electronic structure a notch, since it is not as obvious that the notion of full electron transfer by the rare-earth element is necessarily valid. Indeed, electronic structure calculations frequently suggest significant covalent character in bonds between rare-earth and main-group elements, although the approximation of a trivalent rare-earth cation is still useful.[3,4] New structural features occur, as seen in the rare-earth main-group-element antimonides $LaIn_{0.8}Sb_2$ and $LaSn_{0.75}Sb_2$, which feature strong homoatomic In−In or Sn−Sn bonds, respectively, in one-dimensional chains, as well as extensive multicenter weak Sb−Sb bonds in two-dimensional square nets.[4,5] Extension to the heretofore unexplored *RE*/Ga/Sb system has led to the isolation of two compounds, $La_{13}Ga_8Sb_{21}$ and $Pr_{12}Ga_4Sb_{23}$, which represent the first examples of ternary rare-earth gallium antimonides. Their structures retain the characteristic $GaSb_3$ trigonal planes found in the alkali or alkaline-earth gallium antimonides, but, in a remarkable departure, they also contain puckered Ga_6-rings (in $La_{13}Ga_8Sb_{21}$) or Ga_2-pairs (in $Pr_{12}Ga_4Sb_{23}$) linking extended one-dimensional Sb ribbons. The results confirm earlier expectations for the existence of structures inversely related to a large family of intermetallic structures built up from trigonal prisms, but in which metalloid−metalloid bonding instead of metal−metal bonding is prevalent.[6]

Experimental Section

Synthesis. Starting materials were powders of the rare-earth elements (99.9%, Alfa-Aesar), antimony powder (99.995%, Aldrich), and gallium granules (99.99%, Alfa-Aesar or Cerac). Reactions were carried out on a 0.4 g scale in evacuated fused-silica tubes (8 cm length; 10 mm i.d.). Elemental compositions were determined by EDX (energy-dispersive X-ray) analysis on a Hitachi S-2700 scanning electron microscope. X-ray powder patterns were collected on an Enraf-Nonius FR552 Guinier camera (Cu $K\alpha_1$ radiation; Si standard) and analyzed with the Filmscan and Jade 3.0 software packages.[7]

(1) *Chemistry, Structure, and Bonding of Zintl Phases and Ions*; Kauzlarich, S. M., Ed.; VCH Publishers: New York, 1996.

(2) For example, see the following. (a) $Na_2Ga_3Sb_3$: Cordier, G.; Ochmann, H.; Schäfer, H. *Mater. Res. Bull.* **1986**, *21*, 331. (b) Sr_3GaSb_3: Cordier, G.; Schäfer, H.; Stelter, M. *Z. Naturforsch. B: Chem. Sci.* **1987**, *42*, 1268. (c) $K_{20}Ga_6Sb_{12.66}$: Cordier, G.; Ochmann, H. *Z. Naturforsch. B: Chem. Sci.* **1990**, *45*, 277. (d) Cs_6GaSb_3: Blase, W.; Cordier, G.; Somer, M. *Z. Kristallogr.* **1992**, *199*, 277. (e) $Na_3Sr_3GaSb_4$: Somer, M.; Carrillo-Cabrera, W.; Nuss, J.; Peters, K.; von Schnering, H. G.; Cordier, G. *Z. Kristallogr.* **1996**, *211*, 479. (f) Eisenmann, B.; Cordier, G. In *Chemistry, Structure, and Bonding of Zintl Phases and Ions*; Kauzlarich, S. M., Ed.; VCH Publishers: New York, 1996; p 61.

(3) Papoian, G.; Hoffmann, R. *J. Solid State Chem.* **1998**, *139*, 8.

(4) Ferguson, M. J.; Ellenwood, R. E.; Mar, A. *Inorg. Chem.* **1999**, *38*, 4503.

(5) Ferguson, M. J.; Hushagen, R. W.; Mar, A. *Inorg. Chem.* **1996**, *35*, 4505.

(6) Lam, R.; Mar, A. *Inorg. Chem.* **1998**, *37*, 5364.

10.1021/ic000519w CCC: $19.00
Published on Web 09/09/2000

Table 1. Cell Parameters for Ternary $RE_{12}Ga_4Sb_{23}$ Compounds

compound	a (Å)	b (Å)	c (Å)	V (Å^3)
$La_{12}Ga_4Sb_{23}$	4.344(2)	19.750(7)	26.860(11)	2305(1)
$Ce_{12}Ga_4Sb_{23}$	4.308(2)	19.509(9)	26.667(12)	2241(1)
$Pr_{12}Ga_4Sb_{23}$	4.283(3)	19.394(10)	26.553(16)	2206(1)
$Nd_{12}Ga_4Sb_{23}$	4.268(1)	19.308(6)	26.425(8)	2177.6(8)
$Sm_{12}Ga_4Sb_{23}$	4.213(3)	19.120(10)	26.099(15)	2103(1)

Table 2. Crystallographic Data for $La_{13}Ga_8Sb_{21}$ and $Pr_{12}Ga_4Sb_{23}$

formula	$La_{12.85(1)}Ga_{7.56(6)}Sb_{21}$	$Pr_{12}Ga_{3.98(1)}Sb_{22.90(1)}$
formula mass (amu)	4868.83	4756.48
space group	D_{6h}^1-*P*6/*mmm* (No. 191)	D_{2h}^{25}-*Immm* (No. 71)
a (Å)	17.657(2)[a]	4.2612(3)[b]
b (Å)	17.657(2)[a]	19.4070(13)[b]
c (Å)	4.3378(7)[a]	26.3972(18)[b]
V (Å^3)	1171.2(3)	2183.0(3)
Z	1	2
T (°C)	22	22
λ (Å)	0.710 73	0.710 73
ρ_{calcd} (g cm^{-3})	6.903	7.236
μ(Mo Kα) (cm^{-1})	275.41	293.79
$R(F)$ for $F_o^2 > 2\sigma(F_o^2)$[c]	0.034	0.030
$R_w(F_o^2)$[d]	0.085	0.072

[a] Obtained from a refinement constrained so that $a = b$, $\alpha = \beta = 90°$, and $\gamma = 120°$. [b] Obtained from a refinement constrained so that $\alpha = \beta = \gamma = 90°$. [c] $R(F) = \Sigma||F_o| - |F_c||/\Sigma|F_o|$. [d] $R_w(F_o^2) = [\Sigma[w(F_o^2 - F_c^2)^2]/\Sigma wF_o^4]^{1/2}$; $w^{-1} = [\sigma^2(F_o^2) + (ap)^2 + bp]$ where $p = [\max(F_o^2, 0) + 2F_c^2]/3$. For $La_{13}Ga_8Sb_{21}$, $a = 0.0389$, $b = 0.0000$; for $Pr_{12}Ga_4Sb_{23}$, $a = 0.0302$, $b = 0.0000$.

Single gray needle-shaped crystals of $La_{13}Ga_8Sb_{21}$ (Anal. (mol %): La 34(1), Ga 20(1), Sb 46(1) (average of 2 analyses)) were isolated from a reaction of La, Ga, and Sb in the ratio 1:2:2. The sample was heated at 900 °C for 3 days, cooled slowly to 500 °C over 4 days, and then cooled to 20 °C over 12 h. Numerous attempts at various temperatures and stoichiometries to substitute other rare-earth metals for La in $La_{13}Ga_8Sb_{21}$ were unsuccessful. All of the syntheses resulted, not in the expected $La_{13}Ga_8Sb_{21}$-type phase, but in a different phase, which was subsequently identified as the $Pr_{12}Ga_4Sb_{23}$-type, also crystallizing as gray needles. The single crystals of $Pr_{12}Ga_4Sb_{23}$ (Anal. (mol %): Pr 32(1), Ga 10(1), Sb 58(1) (average of 4 analyses)) used in the structure determination were originally obtained from a reaction of Pr, Ga, and Sb in the ratio 13:8:21 at 1000 °C for 3 days, followed by cooling to 20 °C over 18 h. In contrast to the $La_{13}Ga_8Sb_{21}$-type phase, which could only be prepared with La, rare-earth substitution is possible in $RE_{12}Ga_4Sb_{23}$ (*RE* = La, Ce, Pr, Nd, Sm). Mixtures of the elements *RE*, Ga, and Sb in the stoichiometric ratio 12:4:23, heated as before, resulted in reasonably pure products. The powder patterns of $RE_{12}Ga_4Sb_{23}$ were indexed, and the orthorhombic cell parameters refined with the use of the program POLSQ[8] are given in Table 1.

Structure Determination. Prescreening of crystals of $La_{13}Ga_8Sb_{21}$ and $Pr_{12}Ga_4Sb_{23}$ was important because of their similarity in color and habit. Preliminary cell parameters were obtained from Weissenberg photographs. Final cell parameters for $La_{13}Ga_8Sb_{21}$ and $Pr_{12}Ga_4Sb_{23}$ were determined from least-squares analysis of the setting angles of 1146 or 3256 reflections, respectively, centered on a Bruker P4/RA/SMART-1000 CCD system. Intensity data were collected at 22 °C using a combination of ϕ rotations (0.3°) and ω scans (0.3°) in the range $2° \le 2\theta(\text{Mo K}\alpha) \le 61°$ for $La_{13}Ga_8Sb_{21}$ and $2° \le 2\theta(\text{Mo K}\alpha) \le 66°$ for $Pr_{12}Ga_4Sb_{23}$. Crystal data and further details of the data collections are given in Table 2. All calculations were carried out using the SHELXTL (version 5.1) package.[9] Conventional atomic scattering factors and anomalous dispersion corrections were used.[10] Intensity data were reduced and averaged, and face-indexed numerical absorption corrections were applied in XPREP. Initial atomic positions were located by direct methods using XS, and refinements were performed by least-squares methods using XL.

Weissenberg photographs of $La_{13}Ga_8Sb_{21}$ revealed hexagonal Laue symmetry 6/*mmm* and no systematic extinctions. Upper-level photographs exhibited 6-fold rotational symmetry, ruling out trigonal space groups. On the basis of intensity statistics and the successful structure solution, the centrosymmetric space group *P*6/*mmm* was chosen. Initial positions for all atoms of $La_{13}Ga_8Sb_{21}$, except Ga(2), were found by direct methods. A first refinement revealed considerable electron density at the site ($^1/_3$, $^2/_3$, 0), located at the center of a La_6 trigonal prism and coordinated by three coplanar Sb atoms. This site was assigned to Ga, given the trigonal planar coordination geometry of the site, and reasonable Ga−Sb and Ga−La bond lengths. In early refinements, the thermal ellipsoids for Ga(1) and Ga(2) were quite elongated along the *c*-direction, suggesting that these sites should each be split into two positions. Shifting Ga(1) and Ga(2) off the *x y* $^1/_2$ and *x y* 0 mirror planes, respectively, led to close Ga(1)−Ga(1) and Ga(2)−Ga(2) contacts (0.50 and 0.58 Å), which demand that the Ga(1) and Ga(2) positions each have a maximum occupancy of 50%. Reasonable, if still somewhat elongated, thermal ellipsoids resulted for both atoms. The possibility that the disorder in the Ga positions is a consequence of improper choice of space group was considered; however, the close Ga positions are also present when the structure was refined in lower symmetry space groups such as $P\bar{3}$.

A series of refinements allowing the occupancies of successive atoms to vary freely revealed partial occupancies of 86(1)%, 47.1(5)%, and 47.8(9)% for La(3), Ga(1) and Ga(2), respectively, and essentially full occupancy for all other atoms. The resulting formula is "$La_{12.85(1)}Ga_{7.56(6)}Sb_{21}$" (with $Z = 1$), which is close to the ideal formulation "$La_{13}Ga_8Sb_{21}$" and consistent with EDX analyses. The final refinement for $La_{13}Ga_8Sb_{21}$ led to reasonable values for the anisotropic displacement parameters and a featureless difference electron density map ($\Delta\rho_{max} = 3.80$, $\Delta\rho_{min} = -2.59$ e Å^{-3}).

Weissenberg photographs of $Pr_{12}Ga_4Sb_{23}$ displayed Laue symmetry *mmm* and systematic extinctions (*hkl*: $h + k + l = 2n + 1$) consistent with the orthorhombic space groups *Immm*, *Imm*2, *I*222, and $I2_12_12_1$. Intensity statistics and satisfactory averaging ($R_{int} = 0.044$) favored the centrosymmetric space group *Immm*. Initial positions of all atoms were found by direct methods followed by subsequent difference Fourier syntheses. Once all atomic positions, except for Ga(2), were found, a refinement assuming the ideal formula "$Pr_{12}Ga_4Sb_{23}$" proceeded satisfactorily. However, the difference Fourier map revealed a small amount of residual electron density ($\Delta\rho_{max} = 8.24$, $\Delta\rho_{min} = -2.56$ e Å^{-3}) at a site coordinated by a tetrahedron of Sb atoms (Sb(1) at 2.23(3) Å (×2), Sb(7) at 2.70(4) Å (×2)), analogous to the site partially occupied by Mn atoms in the related structure of La_6MnSb_{15}.[11] This site was assigned to Ga(2), on the basis of the reasonable Ga(2)−Sb(7) and Ga(2)−Pr(1) bond lengths. However, the short Ga(2)−Sb(1) distance precludes the Ga(2) and Sb(1) sites from being simultaneously occupied. The occupancies of Ga(2) and Sb(1) were thus refined with the constraint that their sum be 100% and with the restraint that the displacement parameters be approximately equal (with a standard deviation of 0.003 Å), given significant correlation in the refinement of parameters of closely spaced sites. Refinements in which the occupancies of successive atoms were allowed to vary resulted in essentially 100% occupancy for all atoms, except for Ga(1), Ga(2), and Sb(1), whose occupancies converged to 96.4(7)%, 2.7(2)%, and 97.3(2)%, respectively.

Alternatively, the Ga(2) site may conceivably be assigned to O, since the distance to the two closest Sb(1) atoms is reasonable for an Sb−O bond. Reasonable displacement parameters for O are obtained only if this site is partially occupied (~50%), giving a hypothetical "$Pr_{12}Ga_{3.9}Sb_{23}O$" structure which would have the O atom bridging two Sb atoms of a kinked square sheet. EDX analyses of several $RE_{12}Ga_4Sb_{23}$ crystals

(7) *Filmscan* and *Jade 3.0*; Materials Data Inc.: Livermore, CA, 1996.
(8) POLSQ: Program for least-squares unit cell refinement. Modified by D. Cahen and D. Keszler, Northwestern University, 1983.
(9) Sheldrick, G. M. *SHELXTL*, version 5.1; Bruker Analytical X-ray Systems, Inc.: Madison, WI, 1997.
(10) *International Tables for X-ray Crystallography*; Wilson, A. J. C., Ed.; Kluwer: Dordrecht, The Netherlands, 1992; Vol. C.
(11) Sologub, O.; Vybornov, M.; Rogl, P.; Hiebl, K.; Cordier, G.; Woll, P. *J. Solid State Chem.* **1996**, *122*, 266.

Table 3. Positional and Equivalent Isotropic Displacement Parameters for $La_{13}Ga_8Sb_{21}$ and $Pr_{12}Ga_4Sb_{23}$

atom	Wyckoff position	occupancy	*x*	*y*	*z*	U_{eq} (Å^2)[a]
$La_{13}Ga_8Sb_{21}$						
La(1)	6*m*	1	0.58274(4)	0.16547(8)	$^1/_2$	0.0073(3)
La(2)	6*m*	1	0.16800(4)	0.33600(7)	$^1/_2$	0.0079(3)
La(3)	1*a*	0.859(13)	0	0	0	0.0229(14)
Ga(1)	12*n*	0.471(5)	0.1343(2)	0	0.443(2)	0.030(3)
Ga(2)	4*h*	0.478(9)	$^1/_3$	$^2/_3$	0.0663(11)	0.011(2)
Sb(1)	6*l*	1	0.24818(5)	0.49636(10)	0	0.0086(3)
Sb(2)	6*j*	1	0.24697(7)	0	0	0.0102(3)
Sb(3)	6*k*	1	0.37508(8)	0	$^1/_2$	0.0167(4)
Sb(4)	3*f*	1	$^1/_2$	0	0	0.0088(4)
$Pr_{12}Ga_4Sb_{23}$						
Pr(1)	8*l*	1	0	0.27695(3)	0.40559(2)	0.00798(12)
Pr(2)	8*l*	1	0	0.38900(3)	0.26312(2)	0.00777(11)
Pr(3)	4*j*	1	$^1/_2$	0	0.09340(3)	0.00822(15)
Pr(4)	4*j*	1	$^1/_2$	0	0.38118(3)	0.00953(15)
Ga(1)	4*i*	0.964(7)	0	0	0.18986(7)	0.0225(6)
Ga(2)	4*h*	0.027(2)	0	0.181(3)	$^1/_2$	0.0126(17)
Ga(3)	4*g*	1	0	0.43337(9)	0	0.0134(3)
Sb(1)	8*l*	0.973(2)	0	0.11138(4)	0.43300(3)	0.01520(19)
Sb(2)	8*l*	1	0	0.11584(3)	0.14030(2)	0.00912(13)
Sb(3)	8*l*	1	0	0.22151(3)	0.28669(2)	0.00875(13)
Sb(4)	8*l*	1	0	0.33456(3)	0.14421(2)	0.00908(14)
Sb(5)	4*i*	1	0	0	0.28911(3)	0.00957(18)
Sb(6)	4*h*	1	0	0.38335(5)	$^1/_2$	0.01313(19)
Sb(7)	4*g*	1	0	0.23336(5)	0	0.01133(19)
Sb(8)	2*a*	1	0	0	0	0.0088(2)

[a] U_{eq} is defined as one-third of the trace of the orthogonalized $\mathbf{U}_{ij}$ tensor.

were inconclusive, giving variable O content (from 0 to ~10%) likely arising from surface oxidation of the crystals. However, chemical arguments do not support this model: although several antimonide oxides have been reported, the O atoms in these structures are coordinated to the electropositive metals, never to the more electronegative antimony atoms.[12]

If the original model is accepted, the final formula is "$Pr_{12}Ga_{3.98(1)}Sb_{22.90(1)}$" (with $Z = 2$), close to the ideal formula "$Pr_{12}Ga_4Sb_{23}$" and in excellent agreement with the elemental analysis. The final refinement now led to a featureless electron density map ($\Delta\rho_{max} = 4.79$, $\Delta\rho_{min} = -2.59$ e Å^{-3}) and reasonable displacement parameters for all atoms, except Ga(1). The thermal ellipsoid of this site is somewhat elongated along *a*, suggesting that the Ga(1) atom may be tending to displace randomly slightly above or slightly below the mirror plane at 0 *x y*, a situation similar to, but less pronounced than, that discussed for $La_{13}Ga_8Sb_{21}$ above. Solution of the structure in the lower symmetry space group *I*2*mm* led to a similar elongated thermal ellipsoid for Ga(1), rather than a single well-behaved site.

The atomic positions of $La_{13}Ga_8Sb_{21}$ and $Pr_{12}Ga_4Sb_{23}$ were standardized with the program STRUCTURE TIDY.[13] Final values of the positional and displacement parameters are given in Table 3. Interatomic distances are listed in Table 4. Further data (powder X-ray diffraction data, additional crystal data, and CIFs) are available as Supporting Information, and final structural amplitudes are available from the authors.

Table 4. Selected Interatomic Distances (Å) for $La_{13}Ga_8Sb_{21}$ and $Pr_{12}Ga_4Sb_{23}$

	$La_{13}Ga_8Sb_{21}$		
La(1)−Ga(2)	3.182(3) (×2)	La(3)−Ga(1)	3.051(6) (×6)
La(1)−Sb(4)	3.3326(9) (×2)	La(3)−Ga(1)	3.386(7) (×6)
La(1)−Sb(3)	3.3567(14) (×2)	Ga(1)−Ga(1)	2.422(5) (×2)
La(1)−Sb(1)	3.3749(8) (×4)	Ga(1)−Sb(2)	2.766(7)
La(2)−Sb(1)	3.2737(15) (×2)	Ga(1)−Sb(2)	3.131(7)
La(2)−Ga(1)	3.314(3) (×2)	Ga(2)−Sb(1)	2.6200(16) (×3)
La(2)−Sb(2)	3.3632(6) (×4)	Sb(2)−Sb(3)	3.1338(14) (×2)
La(2)−Sb(3)	3.3648(11) (×2)	Sb(3)−Sb(4)	3.0934(11) (×2)
	$Pr_{12}Ga_4Sb_{23}$		
Pr(1)−Ga(2)	3.11(3)	Pr(4)−Ga(3)	3.3925(10) (×2)
Pr(1)−Sb(2)	3.2150(6) (×2)	Pr(4)−Sb(5)	3.2322(9) (×2)
Pr(1)−Sb(6)	3.2365(8)	Pr(4)−Sb(4)	3.2800(7) (×2)
Pr(1)−Sb(7)	3.2849(4) (×2)	Pr(4)−Sb(1)	3.3290(7) (×4)
Pr(1)−Sb(1)	3.2936(9)	Ga(1)−Sb(2)	2.6011(11) (×2)
Pr(1)−Sb(4)	3.3091(6) (×2)	Ga(1)−Sb(5)	2.620(2)
Pr(1)−Sb(3)	3.3180(8)	Ga(2)−Sb(7)	2.70(4) (×2)
Pr(2)−Ga(1)	3.2743(8) (×2)	Ga(3)−Ga(3)	2.586(4)
Pr(2)−Sb(3)	3.2966(7) (×2)	Ga(3)−Sb(1)	2.9020(7) (×4)
Pr(2)−Sb(3)	3.3095(8)	Sb(1)−Sb(4)	3.1296(7) (×2)
Pr(2)−Sb(4)	3.3119(8)	Sb(3)−Sb(4)	3.0085(7) (×2)
Pr(2)−Sb(2)	3.3239(7) (×2)	Sb(3)−Sb(3)	3.0844(9) (×2)
Pr(2)−Sb(5)	3.3287(6) (×2)	Sb(6)−Sb(8)	3.1088(7) (×2)
Pr(3)−Ga(1)	3.3201(15) (×2)	Sb(6)−Sb(7)	3.1095(10) (×2)
Pr(3)−Sb(8)	3.2585(6) (×2)		
Pr(3)−Sb(2)	3.3356(6) (×4)		
Pr(3)−Sb(6)	3.3472(9) (×2)		

Results and Discussion

Structures. Examples of ternary rare-earth main-group-element antimonides were previously limited to $RE In_{0.8}Sb_2$ and $RE Sn_{0.75}Sb_2$.[4,5] The *RE*/Ga/Sb system is particularly rich, yielding $La_{13}Ga_8Sb_{21}$ and $Pr_{12}Ga_4Sb_{23}$, which are new structure types, in addition to a $RE GaSb_2$ phase, to be reported separately, which is analogous to the In and Sn compounds.[14] The $La_{13}Ga_8Sb_{21}$ phase is distinctly more difficult to prepare than the $Pr_{12}Ga_4Sb_{23}$ phase, requiring an excess of Ga to succeed. There may be structural reasons, evident later, for why this phase could only be prepared for *RE* = La. In contrast, the competing $RE_{12}Ga_4Sb_{23}$ phase forms readily with diverse starting compositions and temperatures. A plot of the unit cell volume for $RE_{12}Ga_4Sb_{23}$ (*RE* = La−Nd, Sm) (Figure 1) shows a monotonic decrease consistent with the lanthanide contraction and a +3 oxidation state for *RE* in all cases.

As shown in Figures 2 and 3, respectively, the structures of $La_{13}Ga_8Sb_{21}$ (down the *c*-axis) and $Pr_{12}Ga_4Sb_{23}$ (down the *a*-axis) bear striking similarities and can be fruitfully discussed together. Both structures contain extended networks of Sb and Ga atoms forming large channels that are occupied by columns of face-sharing trigonal prisms of *RE* atoms. We discuss first

(12) Brock, S. L.; Kauzlarich, S. M. *Comments Inorg. Chem.* **1995**, *17*, 213.
(13) Gelato, L. M.; Parthé, E. *J. Appl. Crystallogr.* **1987**, *20*, 139.
(14) Mills, A. M.; Mar, A. Manuscript in preparation.

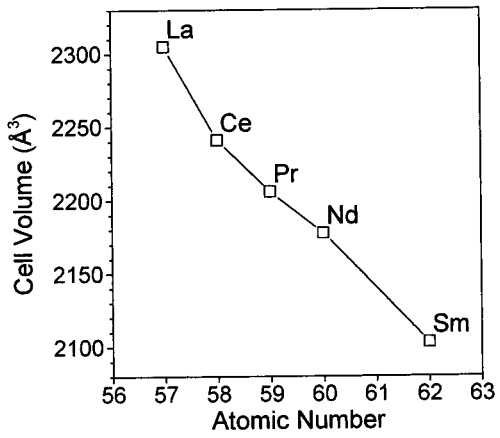

Figure 1. Plot of unit cell volume for $RE_{12}Ga_4Sb_{23}$ compounds. The lines are drawn only for guidance.

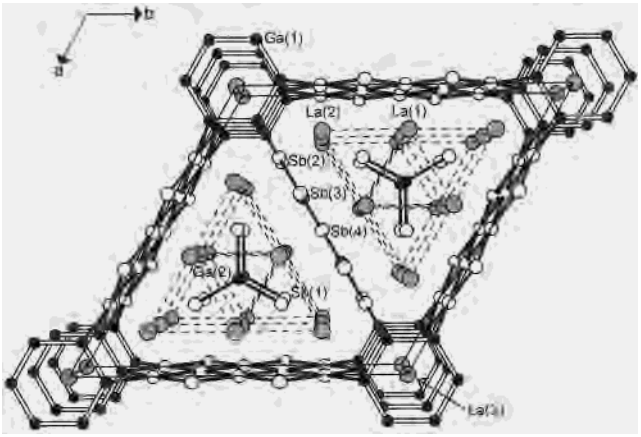

Figure 2. View of $La_{13}Ga_8Sb_{21}$ down the *c*-axis showing the unit cell outline and the labeling scheme. The large lightly shaded circles are La atoms, the small solid circles are Ga atoms, and the medium open circles are Sb atoms. The dashed lines merely outline the assemblies of La_6 trigonal prisms.

the overall connectivity in these structures, and then consider in turn the coordination around the Sb, Ga, and *RE* atoms.

In $La_{13}Ga_8Sb_{21}$ (Figure 2), the channels are outlined by 21-membered rings which are formed by five-atom-wide ribbons of Sb atoms (Sb(2)−Sb(3)−Sb(4)−Sb(3)−Sb(2)) that are bordered by Ga(1) atoms and linked by Ga(1)−Ga(1) bonds. The Ga(1)−Ga(1) bonds result in puckered Ga_6-rings which sandwich La(3) atoms at the origin of the unit cell. Four trigonal prisms whose vertices are La(1) and La(2) atoms share rectangular faces to form a larger triangular assembly residing within the channels. The three outer trigonal prisms are filled by Sb(1) atoms, while the central prism is filled by a Ga(2) atom, generating trigonal planar $GaSb_3$ units. These trigonal prismatic columnar assemblies $^1_\infty[La_6GaSb_3]$ extend along the *c*-direction such that they are in registry with each other in adjacent channels, the La atoms being positioned directly across each other on opposite sides of common square faces within the Sb ribbons.

The change from the hexagonal symmetry of $La_{13}Ga_8Sb_{21}$ (Figure 2) to the pseudohexagonal orthorhombic symmetry of $Pr_{12}Ga_4Sb_{23}$ (Figure 3) results from a loss of equivalence in the three Ga/Sb segments that together outline the anionic channels, as shown in Figure 4. The channels within $Pr_{12}Ga_4Sb_{23}$ are also enclosed by 21 atoms, but now they are built up from isolated five-atom-wide Sb ribbons (Sb(7)−Sb(6)−Sb(8)−Sb(6)−Sb(7)) and six-atom-wide Sb ribbons (Sb(1)−Sb(4)−Sb(3)−Sb(3)−Sb(4)−Sb(1)) that are connected by Ga(3) atoms. The five-atom-wide Sb ribbons are parallel to (001), and the six-atom-wide Sb ribbons are approximately parallel to (011) or (01$\bar{1}$). The topological transformation involves taking the Ga atoms that border one of the five-atom-wide Sb ribbons in $La_{13}Ga_8Sb_{21}$ (Figure 4a) and twisting them outward to form the isolated five-atom-wide Sb ribbons in $Pr_{12}Ga_4Sb_{23}$ (Figure 4b). Note that Ga atoms are also replaced by Sb atoms to form the six-atom-wide Sb ribbons in $Pr_{12}Ga_4Sb_{23}$. Another way to consider part of the anionic substructure in $Pr_{12}Ga_4Sb_{23}$ is through the stacking of strongly kinked two-dimensional Sb square sheets perpendicular to the *b*-direction; where the folds occur to produce the kinks, Sb atoms are replaced by Ga atoms. The kinked sheets are then linked by Ga(3)−Ga(3) bonding, completing the channels. In $Pr_{12}Ga_4Sb_{23}$, Ga_2-*pairs* occur, in contrast to the Ga_6-*rings* in $La_{13}Ga_8Sb_{21}$. The channels of $Pr_{12}Ga_4Sb_{23}$ enclose columns of four trigonal prisms that have Pr atoms (Pr(1), Pr(2), Pr(3), Pr(4)) at their vertices and that are grouped together in the same manner as in $La_{13}Ga_8Sb_{21}$. Likewise, the Pr_6 trigonal prisms are filled by Ga(1), Sb(5), and two Sb(2) atoms that together constitute trigonal planar $GaSb_3$ units. However, in $Pr_{12}Ga_4Sb_{23}$, the $^1_\infty[Pr_6GaSb_3]$ columnar assemblies are shifted by half the unit cell length along *a* with respect to each other in adjacent channels separated by the six-atom-wide Sb ribbons

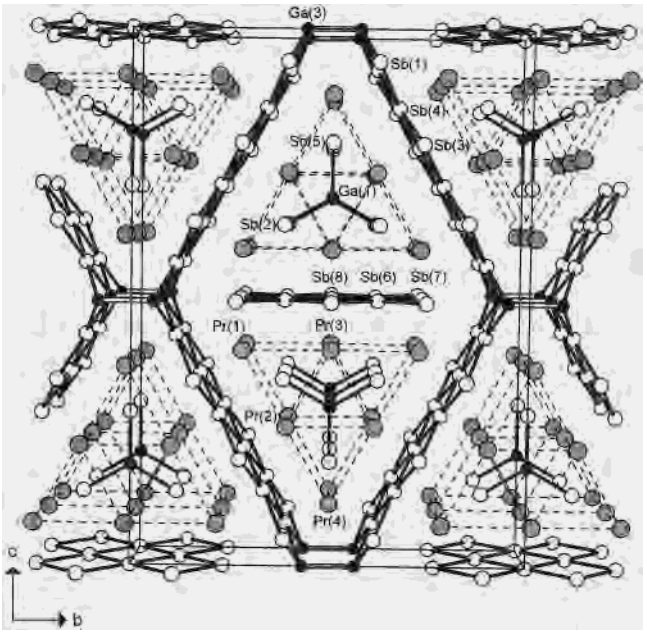

Figure 3. View of $Pr_{12}Ga_4Sb_{23}$ down the *a*-axis showing the unit cell outline and the labeling scheme. The large lightly shaded circles are Pr atoms, the small solid circles are Ga atoms, and the medium open circles are Sb atoms. The dashed lines merely outline the assemblies of Pr_6 trigonal prisms.

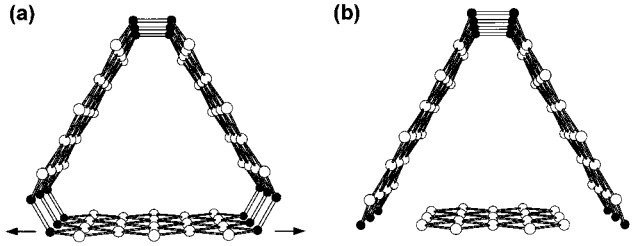

Figure 4. Comparison of the 21-atom channels in (a) $La_{13}Ga_8Sb_{21}$, composed of five-atom-wide Sb ribbons, and (b) $Pr_{12}Ga_4Sb_{23}$, composed of two six-atom-wide Sb ribbons and one five-atom-wide Sb ribbon. These Sb ribbons are linked by Ga atoms.

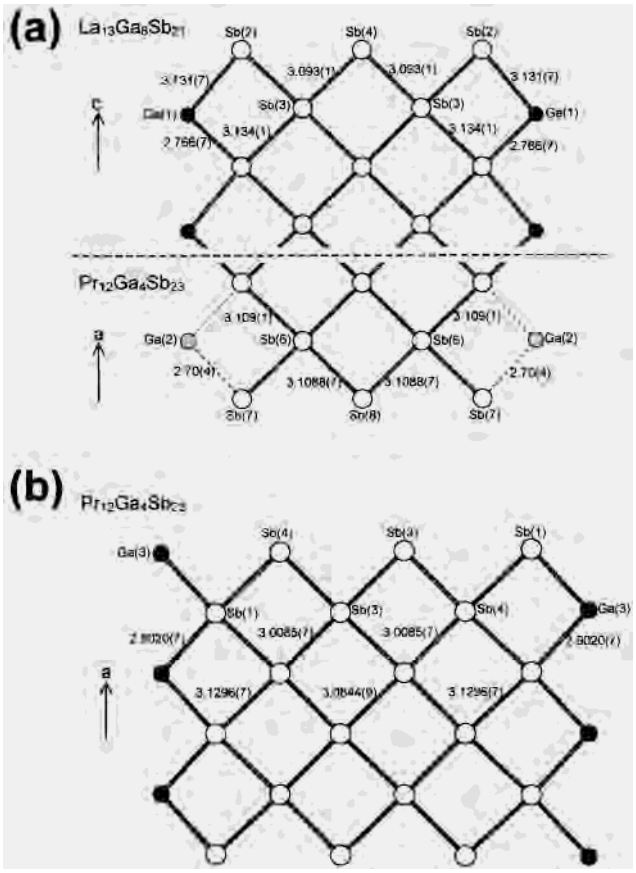

Figure 5. Comparison of (a) the five-atom-wide Sb ribbons in $La_{13}Ga_8Sb_{21}$ and $Pr_{12}Ga_4Sb_{23}$ and (b) the six-atom-wide Sb ribbon in $Pr_{12}Ga_4Sb_{23}$, viewed perpendicular to their axes of infinite extension. The ribbons are bounded on two sides by Ga atoms, but in the case of the five-atom-wide Sb ribbon in $Pr_{12}Ga_4Sb_{23}$, the Ga(2) site is only occupied at 2.7(2)%. Bond lengths in Å are indicated.

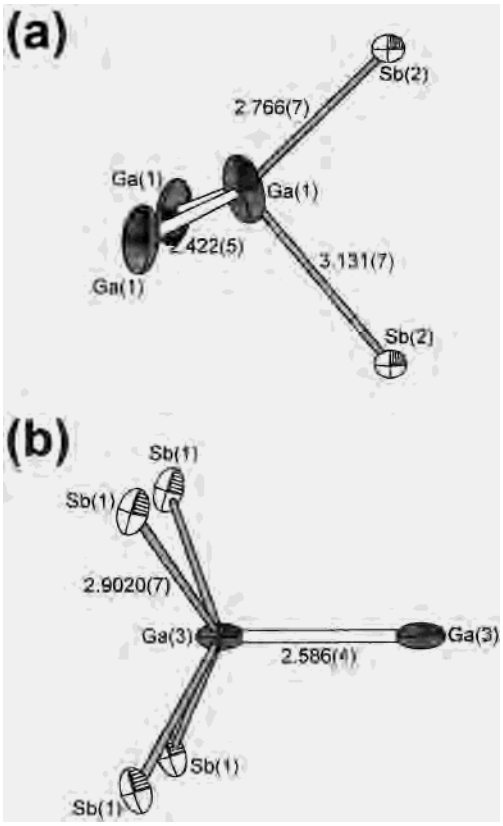

Figure 6. (a) Distorted tetrahedral coordination around Ga(1) in $La_{13}Ga_8Sb_{21}$. (b) Square pyramidal coordination around Ga(3) in $Pr_{12}Ga_4Sb_{23}$. Bond lengths in Å are indicated.

of the kinked sheets. Correspondingly, the Pr atoms on opposite sides of the kinked sheets are positioned in an alternating "checkerboard" fashion, an arrangement in which no two Pr atoms share the same square face. With respect to the isolated five-atom-wide Sb ribbon, the $^1_\infty[Pr_6GaSb_3]$ columnar assemblies across each other remain in registry and the Pr atoms are situated directly across each other on opposite sides of square faces.

The one-dimensional five- or six-atom-wide Sb ribbons that enclose the channels in $La_{13}Ga_8Sb_{21}$ and $Pr_{12}Ga_4Sb_{23}$ may be viewed as segments cut from the infinite two-dimensional square nets of Sb atoms commonly found in many binary and ternary antimonides. Five-atom-wide Sb ribbons occur in both $La_{13}Ga_8Sb_{21}$ and $Pr_{12}Ga_4Sb_{23}$, but the Sb−Sb bonds follow a long−short−short−long pattern in $La_{13}Ga_8Sb_{21}$, while they are essentially identical in $Pr_{12}Ga_4Sb_{23}$ (Figure 5a). Six-atom-wide Sb ribbons occur in $Pr_{12}Ga_4Sb_{23}$, where the Sb−Sb bonds follow an alternating long−short−long−short−long pattern (Figure 5b). These Sb−Sb distances, which range from 3.0085(7) to 3.134(1) Å, are longer than the intralayer Sb−Sb single-bond length (2.908 Å) and shorter than the weakly bonding interlayer distance (3.355 Å) in elemental Sb.[15] Rather, they are comparable to the Sb−Sb distances occurring in the Sb square sheets in $LaSb_2$ (3.087−3.157 Å),[16] $LaIn_{0.8}Sb_2$ (3.119(3)−3.142(3) Å),[4] or $LaZn_{0.52}Sb_2$ (3.097(2) Å),[17] which have been interpreted as one-electron half-bonds.[4,5] Gallium atoms are then located at the fringes of these five- or six-atom-wide Sb ribbons so that they may be considered to be the terminal atoms of seven- or eight-atom-wide ribbons, respectively. In the case of $Pr_{12}Ga_4Sb_{23}$, the Ga(2) site is occupied to such a small extent (2.7(2)%) that the description of isolated five-atom-wide Sb ribbons made earlier is probably more useful, although for the purpose of comparison, they are portrayed in Figure 5a.

In $La_{13}Ga_8Sb_{21}$, Ga(1) resides at a site that is 0.50 Å distant from a symmetry-equivalent position across a mirror plane, so that only one of these can be occupied locally. One short (2.766(7) Å) and one long (3.131(7) Å) Ga(1)−Sb(2) bond form (Figure 5a). Each Ga(1) atom is additionally coordinated to two other Ga(1) atoms of neighboring ribbons to complete a distorted $Ga(Ga_2Sb_2)$ tetrahedron (Figure 6a). The shorter Ga(1)−Sb(2) distance is slightly greater than the Ga−Sb single-bond distances observed in the isolated $GaSb_4^{9-}$ tetrahedra found in the Zintl phase $Na_3Sr_3GaSb_4$ (2.709(2)−2.752(5) Å)[2e] or in the corner-sharing $GaSb_4$ tetrahedra found in GaSb (2.64 Å).[18] However, the longer Ga(1)−Sb(2) distance must indicate a considerably weaker bonding interaction. Together, these two contacts may be viewed as a 3-center-2-electron bond with unequal distribution of electron density between the three atoms. The Ga(1)−Ga(1) bonding that connects adjacent Sb ribbons results in a Ga_6-ring (Figure 8). It is assumed that the Ga_6-ring adopts a chair conformation (Ga−Ga−Ga 115.9(3)°) since this choice of local site occupation leads to intra-ring Ga(1)−Ga(1) distances of 2.422(5) Å, precluding the unreasonably shorter

(15) Donohue, J. *The Structures of the Elements*; Wiley: New York, 1974.
(16) Wang, R.; Steinfink, H. *Inorg. Chem.* **1967**, *6*, 1685.
(17) Cordier, G.; Schäfer, H.; Woll, P. *Z. Naturforsch. B: Anorg. Chem. Org. Chem.* **1985**, *40*, 1097.
(18) Straumanis, M. E.; Kim, C. D. *J. Appl. Phys.* **1965**, *36*, 3822.

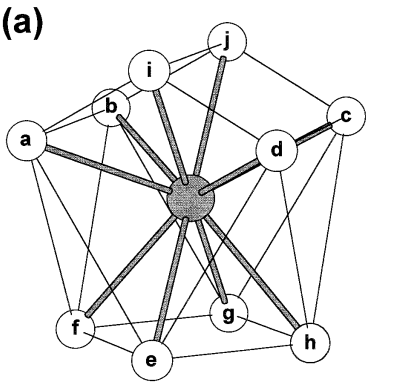

site	coordination environment		
central	La(1)	Pr(2)	Pr(3)
a–h	Sb	Sb	Sb
i–j	Ga (split)	Ga	Ga

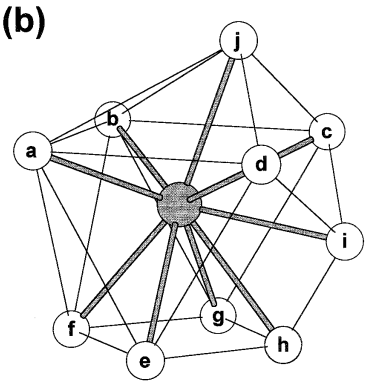

site	coordination environment		
central	La(2)	Pr(1)	Pr(4)
a–g, j	Sb	Sb	Sb
h	Ga (split)	Sb (97.3%)	Ga
i	Ga (split)	Ga (2.7%)	Ga

Figure 7. Coordination environments around La atoms in $La_{13}Ga_8Sb_{21}$ or Pr atoms in $Pr_{12}Ga_4Sb_{23}$. Sites a−h define a square antiprism, which is capped by additional atoms at sites i and j above (a) one square face or (b) one square and one triangular face.

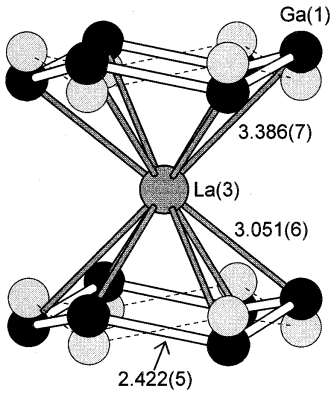

Figure 8. Coordination environment around La(3), sandwiched by two puckered Ga_6-rings, in $La_{13}Ga_8Sb_{21}$. The Ga(1) sites are approximately 50% occupied.

2.371(4) Å distances that would occur in any other ring conformation. Even the 2.422(5) Å Ga(1)−Ga(1) distance is somewhat shorter than the Ga−Ga distances found in GaTe (2.431(2)−2.437(3) Å)[19] or the intermetallic compounds $LaGa_2$ (2.494 Å)[20] and $Na_{22}Ga_{39}$ (2.435(7)−2.989(7) Å).[21] However, single Ga−Ga distances as short as 2.333(1) Å (in [(ᵗBu)NCHCHN(ᵗBu)]GaGa[(ᵗBu)NCHCHN(ᵗBu)])[22] have been observed in organometallic complexes. The occurrence of this unusually short Ga−Ga bond may explain why the $La_{13}Ga_8Sb_{21}$ phase has only been found with the largest *RE* so far. Substitution of a smaller *RE* for La would contract the structure and shrink the $^1_\infty[RE_6GaSb_3]$ columnar assemblies to such an extent that the Ga−Ga bonds linking the Sb ribbons would become unreasonably short. In the $Pr_{12}Ga_4Sb_{23}$ structure, the Ga−Sb bonds at two corners of the channels have been broken, and only one Ga−Ga bond remains (Figure 4); the relaxed steric requirements permit a larger range of *RE* trigonal prism sizes within the channels.

In $Pr_{12}Ga_4Sb_{23}$, Ga(3) is bonded to four Sb(1) atoms at a distance of 2.9020(7) Å, which is longer than typical Ga−Sb single bonds in Zintl compounds,[2] but is consistent with a Ga−Sb half-bond, analogous to one-electron Sb−Sb bonds within square sheets. The Ga_2-pairs which link together kinked sheets are formed when Ga(3) bonds with a neighboring Ga(3) atom at a distance of 2.586(4) Å, longer than that found in $La_{13}Ga_8Sb_{21}$, but comparable to typical values in other solid-state compounds (e.g., 2.541(3) Å in $Na_2Ga_3Sb_3$).[2a] These coordinating atoms around Ga(3) thus complete a $Ga(GaSb_4)$ square pyramid, with Ga at the apical and Sb at the basal positions (Figure 6b). For comparison, a $GaGa_5$ square pyramidal coordination is encountered in binary $BaAl_4$-type gallide phases such as $BaGa_4$.[23] It has been proposed that, in $BaGa_4$, a full single bond forms to the apical Ga atom, but multicenter bonding takes place to the four basal Ga atoms in a $GaGa_5$ square pyramid, a bonding situation similar to the suggestion above for the $Ga(GaSb_4)$ square pyramid in $Pr_{12}Ga_4Sb_{23}$.[24−26]

Common to both $La_{13}Ga_8Sb_{21}$ and $Pr_{12}Ga_4Sb_{23}$ are the $GaSb_3$ units which result from filling the RE_6 trigonal prisms (Figures 2 and 3). Similarly filled four-prism assemblies are found in the Zintl compound Cs_6GaSb_3,[2d] while larger filled nine-prism assemblies are found in $K_{10}Ga_3Sb_{6.33}$.[2c] The Ga−Sb bond distances of the $Ga(2)Sb(1)_3$ unit of $La_{13}Ga_8Sb_{21}$ (2.6200(16) Å) and the $Ga(1)Sb(2)_2Sb(5)$ unit of $Pr_{12}Ga_4Sb_{23}$ (2.6011(11)−2.620(2) Å) are comparable to those of the trigonal planar $GaSb_3^{6-}$ units found in Cs_6GaSb_3 (2.608(5)−2.676(5) Å)[2d] and of the cyclic $Ga_3Sb_6^{9-}$ anions found in $K_{20}Ga_6Sb_{12.66}$ (2.552(4)−2.632(4) Å).[2c] Three-coordinate gallium may seem unusual in other contexts, but does occur in many of the alkali or alkaline-earth metal gallium antimonides. Partial double-bond character has been invoked to explain the somewhat shorter Ga−Sb bonds in the trigonal planar $GaSb_3$ units of these compounds.[2c] It must be realized that the surrounding *RE* atoms will also no doubt exert strong matrix effects. However, unlike the anions in these Zintl compounds which are rigorously planar, the Ga atoms of the $GaSb_3$ units in $La_{13}Ga_8Sb_{21}$ and $Pr_{12}Ga_4Sb_{23}$ are shifted slightly above or below the plane of the Sb atoms. Two

(19) Julien-Pouzol, M.; Jaulmes, S.; Guittard, M.; Alapini, F. *Acta Crystallogr. Sect. B: Struct. Crystallogr. Cryst. Chem.* **1979**, *35*, 2848.
(20) Kimmel, G.; Dayan, D.; Zevin, L.; Pelleg, J. *Metall. Trans. A* **1985**, *16*, 167.
(21) Ling, R. G.; Bélin, C. *Acta Crystallogr. Sect. B: Struct. Crystallogr. Cryst. Chem.* **1982**, *38*, 1101.
(22) Brown, D. S.; Decken, A.; Cowley, A. H. *J. Am. Chem. Soc.* **1995**, *117*, 5421.
(23) Bruzzone, G. *Boll. Sci. Fac. Chim. Ind. Bologna* **1966**, *24*, 113.
(24) Zheng, C.; Hoffmann, R. *Z. Naturforsch. B: Anorg. Chem. Org. Chem.* **1986**, *41*, 292.
(25) Burdett, J. K.; Miller, G. J. *Chem. Mater.* **1990**, *2*, 12.
(26) Häussermann, U.; Nesper, R. *J. Alloys Compd.* **1995**, *218*, 244.

close Ga(2) positions, each approximately 0.3 Å off the plane of the Sb atoms, are resolved in $La_{13}Ga_8Sb_{21}$, while in $Pr_{12}Ga_4Sb_{23}$, this tendency toward pyramidalization is expressed as an elongated Ga(1) thermal ellipsoid. Such behavior may imply that additional electron density is localized at the Ga centers in question.

The *RE* atoms at the vertices of the trigonal prisms share similar coordination numbers (CN 9 or 10) and environments in both $La_{13}Ga_8Sb_{21}$ and $Pr_{12}Ga_4Sb_{23}$. As is typical in ternary rare-earth antimonides containing Sb square sheets, the *RE* atoms reside at the centers of capped square antiprisms.[4,5,11,16,17] With a−h designating the eight corners of a square antiprism, two additional coordinating sites i and j are found, either both capping the same square face (Figure 7a) or one capping a square face and another capping a triangular face of the square antiprism (Figure 7b). The *RE* environments then differ in the placement and identity of coordinating atoms. In the first type of arrangement, which applies to La(1) in $La_{13}Ga_8Sb_{21}$ and to Pr(2) and Pr(3) in $Pr_{12}Ga_4Sb_{23}$, two Ga atoms cap one square face of a square antiprism of Sb atoms. The Ga sites around La(1) are split in a manner reminiscent of the situation in $LaSn_{0.75}Sb_2$, where the capping Sn atom can reside in several closely spaced partially occupied sites.[5] In the second type of arrangement, atoms from a Ga_2-pair occupy sites h and i, forcing an Sb atom to occupy the capping site j in the square antiprisms around La(2) in $La_{13}Ga_8Sb_{21}$ and Pr(4) in $Pr_{12}Ga_4Sb_{23}$. In the case of Pr(1), h and i are too close for them to be occupied simultaneously by Sb and Ga, respectively; if site i is ignored, then the commonly observed nine-coordinate monocapped square antiprism of Sb atoms results. The *RE*−Sb and *RE*−Ga distances (Table 4) in both structures are reasonable when compared with those found in the binary compounds $LaSb_2$ (3.183−3.432 Å),[16] $PrSb_2$ (3.151−3.377 Å),[27] $LaGa_2$ (3.335 Å),[20] and $PrGa_2$ (3.278 Å).[28]

The coordination environment of La(3), which is sandwiched between Ga_6-rings at the origin of the unit cell in $La_{13}Ga_8Sb_{21}$, is quite different from the square antiprismatic geometries of the other *RE* atoms in the structure. Each La(3) atom is coordinated by 12 Ga(1) atoms of two puckered Ga_6-rings, six at the short distance of 3.051(6) Å and six at the longer distance of 3.386(7) Å (Figure 8). Assuming that the Ga_6-rings adopt a chair conformation, two possibilities exist for the local coordination geometry of La(3). The puckered rings may be parallel, with all inter-ring Ga(1)−Ga(1) distances being 4.338(9) Å; this arrangement is similar to that found in the $CeCd_2$ structure type adopted by Gd_5CuGa_9.[29] Alternatively, the rings may be inverted with respect to one another, in such a manner that three short (3.843(8) Å) and three long inter-ring Ga(1)−Ga(1) distances result. Although this relative ring orientation resembles that between the puckered 6^3 layers of the $CaIn_2$ structure type, the shortest inter-ring Ga(1)−Ga(1) distance is much longer than the bonding interlayer Ga−Ga distance of 2.961 Å found in $CaIn_2$-type $YbGa_2$.[30] It is unclear whether the disorder results from a random occupation of the Ga(1) sites without any preferred relative ring orientation, or whether local ordering exists along each 6-fold axis (with the Ga_6-rings all either parallel or inverted) and the disorder results from the random distribution of these axes.

Bonding. The variety of main-group element substructures present in these rare-earth gallium antimonides, absent in the alkali or alkaline-earth gallium antimonides, is remarkable. It is of interest to see how far the Zintl concept can be used to account for these complex substructures, especially given the presence of nonclassical bonding patterns such as the Sb ribbons. Inherent in the Zintl concept is the assumption that full electron transfer takes place from the electropositive to the electronegative elements, but it would be thought that this is rendered less applicable because of the reduced electronegativity differences between rare-earth and main-group elements (compared to electronegativity differences between alkali or alkaline-earth elements and main-group elements).

Assuming, then, that the rare-earth atoms adopt a +3 oxidation state, the donated electrons contribute to the formation of bonds in the remaining framework, giving the formulations $(La^{3+})_{13}[Ga_8Sb_{21}]^{39-}$ and $(Pr^{3+})_{12}[Ga_4Sb_{23}].^{36-}$ The ambiguity lies in the valence state of the Ga atoms, so we will satisfy closed-shell requirements for the more electronegative Sb atoms first. Any electrons that remain once the Sb octets have been satisfied may then be used by the Ga atoms, either as lone pairs or for homoatomic Ga−Ga bonding. Three types of Sb atoms are present in both structures: isolated Sb^{3-} atoms centering the RE_6 trigonal prisms, interior Sb^{1-} atoms participating in four Sb−Sb half-bonds within the ribbons, and terminal Sb^{2-} atoms participating in only two Sb−Sb half-bonds at the ribbon edges. The idea of weak one-electron Sb−Sb bonds has now gained acceptance and is supported on firm theoretical grounding.[3−5,31] As shown earlier in Figure 5, there is some distortion of the Sb atoms away from ideal square planar geometries. A similar, but more asymmetrical, pattern is observed in the narrower, three-atom-wide Sb ribbons found in La_6MnSb_{15} and has been traced to a second-order Peierls distortion.[3,11] It is likely that a similar electronic driving force is responsible for the distortions of the five- and six-atom-wide Sb ribbons in $La_{13}Ga_8Sb_{21}$ and $Pr_{12}Ga_4Sb_{23}$, although understanding the more complicated patterns found here will require a more detailed analysis.

In our electron-counting exercise, we now arrive at the formulations $[(La^{3+})_{13}(Ga^0)_8(Sb^{3-})_6(Sb^{2-})_6(Sb^{1-})_9]$ and $[(Pr^{3+})_{12}(Ga^{1.25+})_4(Sb^{3-})_6(Sb^{2-})_6(Sb^{1-})_{11}]$. In the case of $La_{13}Ga_8Sb_{21}$, the Ga atoms of $La_{13}Ga_8Sb_{21}$ must have an oxidation state of 0, on average, in order to maintain charge balance. This implies that 24 electrons (3 electrons/Ga atom × 8 Ga atoms) are distributed over the six Ga(1) and two Ga(2) atoms per formula unit. Twelve of these electrons are used to form the six single bonds of the $Ga(1)_6$-rings. For the problem of localizing the 12 remaining electrons (or 1.5 electrons/Ga atom), perhaps some provocative suggestions can be made. The Ga−Ga distance within the $Ga(1)_6$-rings is short (2.422(5) Å) and is comparable to the value of 2.420(1) Å found in $[(^tBu_3Si)_2GaGa(Si^tBu_3)]$ or 2.441(1) Å found in the cyclic molecule $[\{(Mes_2C_6H_3)Ga\}_3]^{2-}$, where formal Ga−Ga bond orders of 1.5 and 1.33, respectively, are proposed and partial π-overlap is presumably involved.[32−34] Equally, π-overlap may be involved in the Ga−Sb bonds of the trigonal planar $GaSb_3$ units.[2c] As well, the tetrahedral or trigonal planar coordination geometries of Ga(1) and Ga(2), respectively, are both distorted in a manner that could indicate

(27) Abdusalyamova, M. N.; Rahmatov, O. I.; Faslyeva, N. D.; Tchuiko, A. G. *J. Less-Common Met.* **1988**, *141*, L23.
(28) Ball, A. R.; Gignoux, D.; Schmitt, D. *J. Magn. Magn. Mater.* **1993**, *119*, 96.
(29) Dwight, A. E. *Rare Earths Mod. Sci. Technol.* **1980**, *2*, 39.
(30) Iandelli, A. *Z. Anorg. Allg. Chem.* **1964**, *330*, 221.
(31) Brylak, M.; Jeitschko, W. *Z. Naturforsch. B: Chem Sci.* **1994**, *49*, 747.
(32) Wiberg, N.; Amelunxen, K.; Nöth, H.; Schwenk, H.; Kaim, W.; Klein, A.; Scheiring, T. *Angew. Chem., Int. Ed. Engl.* **1997**, *36*, 1213.
(33) Li, X.-W.; Pennington, W. T.; Robinson, G. H. *J. Am. Chem. Soc.* **1995**, *117*, 7578.
(34) (a) Power, P. P. *J. Chem. Soc., Dalton Trans.* **1998**, 2939. (b) Power, P. P. *Chem. Rev.* **1999**, *99*, 3463.

the stereochemical activity of a lone pair of electrons. Lastly, further reduction of the Sb ribbons is possible without severe structural consequences, since the square nets from which they are excised can act as electron "sinks",[35] effectively allowing Sb−Sb bond orders that need not be exactly 0.5.

In the case of $Pr_{12}Ga_4Sb_{23}$, the Ga atoms must have an average oxidation state of +1.25. Seven electrons (1.75 electrons/Ga atom × 4 Ga atoms) are distributed over the two Ga(1) and two Ga(3) atoms per formula unit. Two of these electrons form the Ga(3)−Ga(3) single bond that links the kinked Sb sheets. Five electrons (1.25 electrons/Ga atom) remain. As in the case of $La_{13}Ga_8Sb_{21}$, the distribution of these remaining electrons, whether localized on Ga(1) and Ga(3), or participating in further orbital overlap, cannot be determined conclusively at this stage. It is hoped that electronic band structure calculations will clarify this picture. However, extrapolating from the electronic structure of the related La_6MnSb_{15}, where kinked Sb square sheets are also found, leads to a simple explanation for why the corresponding sheets in $Pr_{12}Ga_4Sb_{23}$ are kinked only where Ga has been substituted for Sb.[3] Atoms residing at the kinked sites have some degree of sp hybridization. Since lighter elements undergo such hybridization more readily than heavier elements (the usually cited reason of closer energetic separation of s and p orbitals is disputable),[34,36] it is not surprising that the Ga atoms are the ones occupying the kinked sites instead of Sb atoms in the square sheets.

Structural Relationships. Superficially, the structures of $La_{13}Ga_8Sb_{21}$ and $Pr_{12}Ga_4Sb_{23}$ resemble the hexagonal structures of a large family of metal-rich compounds, generally phosphides and silicides, composed of differently sized triangular groupings of trigonal prisms.[37−39] The $Ho_6Ni_{20}P_{13}$ structure ($P6_3/m$)[40] and its antitype $Ba_{0.8}Hf_{12}As_{17.7}$ ($P6_3/m$)[6] are most similar to $La_{13}Ga_8Sb_{21}$ and $Pr_{12}Ga_4Sb_{23}$: all four structures contain four-prism-large triangular assemblies of trigonal prisms separated by ribbons cut from square nets. Generally, metal−metal bonding networks predominate in compounds such as $Ho_6Ni_{20}P_{13}$,[40] but in $La_{13}Ga_8Sb_{21}$ and $Pr_{12}Ga_4Sb_{23}$ we see the emergence of inversely related structures, first recognized in $Ba_{0.8}Hf_{12}As_{17.7}$, in which metalloid−metalloid (As−As or Sb−Sb) bonding is a prominent feature.[6]

There exists a simpler structure, $Cs_6SnAs_3O_{0.5}$, in which assemblies of four trigonal prisms appear (Figure 9a).[41] In $Ba_{0.8}Hf_{12}As_{17.7}$ (Figure 9b) and $La_{13}Ga_8Sb_{21}$ (Figure 9c), however, extended hexagonal channel networks of As−As or Sb−Sb bonds, respectively, separate the trigonal prism assemblies. In $Ba_{0.8}Hf_{12}As_{17.7}$, six-atom-wide ribbons of As atoms form 18-atom channels that enclose assemblies of Hf_6 trigonal prisms, the outermost ones being filled by As atoms and the central one vacant. The effect of the 6_3 screw axes present in $Ba_{0.8}Hf_{12}As_{17.7}$ is to translate neighboring columnar assemblies of Hf_6 trigonal prisms by $c/2$ along the column axis with respect to one another. Likewise, the As ribbons are also mutually displaced. In $La_{13}Ga_8Sb_{21}$, seven-atom-wide ribbons composed of Sb and Ga separate triangular groupings of larger La_6 prisms.

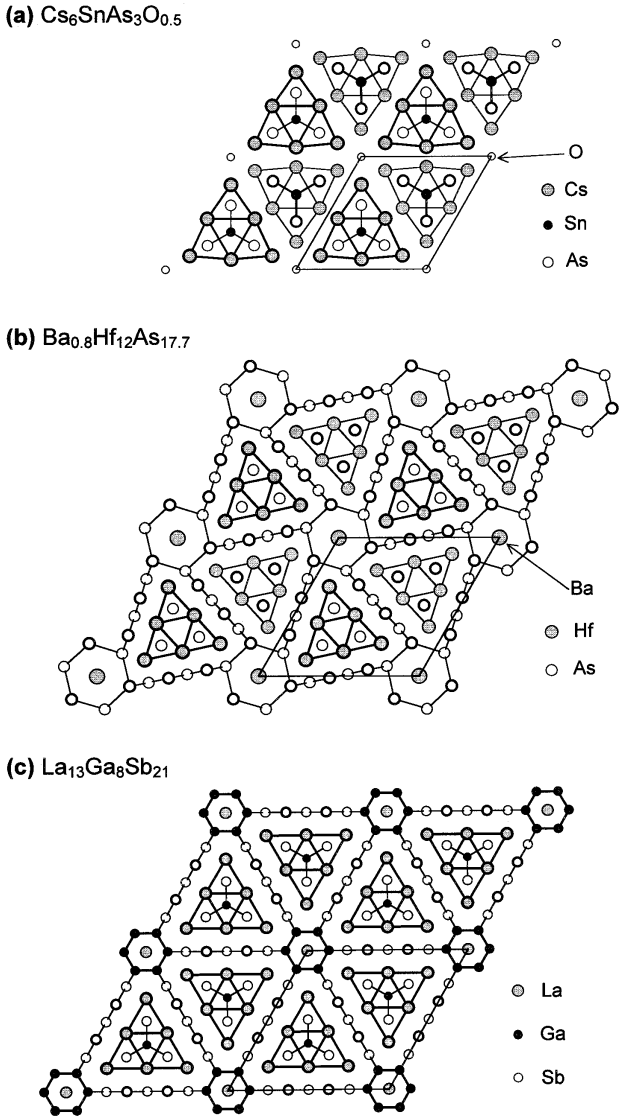

Figure 9. Comparison of the hexagonal structures of (a) $Cs_6SnAs_3O_{0.5}$, (b) $Ba_{0.8}Hf_{12}As_{17.7}$, and (c) $La_{13}Ga_8Sb_{21}$ shown in projection down the *c*-axis. Circles with thicker rims are atoms residing in planes displaced by $c/2$.

In contrast to $Ba_{0.8}Hf_{12}As_{17.7}$, the structure of $La_{13}Ga_8Sb_{21}$ does not contain a 6_3-axis and, consequently, there is no mutual displacement of the Ga/Sb ribbons. This arrangement of the ribbons results in a near-planar Ga_6-ring around each corner of the unit cell. It also forces the La atoms on either side of the ribbons to share the same square face of atoms, preventing any translation of the assemblies of trigonal prisms relative to one another.

The structure of $Pr_{12}Ga_4Sb_{23}$ is more closely related to the La_6MnSb_{15} structure type adopted by RE_6MSb_{15} (RE = La, Ce; M = Mn, Cu, Zn).[11] The single-prism columns of La_6 trigonal prisms that are filled by isolated Sb atoms in La_6MnSb_{15} (Figure 10a) are replaced by larger four-prism triangular groupings in $Pr_{12}Ga_4Sb_{23}$ (Figure 10b). A corresponding enlargement of the pseudohexagonal channels surrounding the column of trigonal prisms in La_6MnSb_{15} also takes place. The two-dimensional Sb sheets of La_6MnSb_{15} are folded at every fifth diagonal to allow intersheet Sb−Sb bonding, while in $Pr_{12}Ga_4Sb_{23}$, kinks in the sheets occur along every seventh diagonal, where Ga atoms replace Sb atoms. The three-atom-wide Sb ribbons in La_6MnSb_{15} (drawn isolated in Figure 10a) are replaced by five-atom-wide Sb ribbons in $Pr_{12}Ga_4Sb_{23}$. In La_6MnSb_{15}, there are Mn atoms

(35) Ferguson, M. J.; Hushagen, R. W.; Mar, A. *J. Alloys Compd.* **1997**, *249*, 191.
(36) Kutzelnigg, W. *Angew. Chem., Int. Ed. Engl.* **1984**, *23*, 272.
(37) Gladyshevskii, E. I.; Grin, Yu. N. *Sov. Phys.—Crystallogr. (Transl. Kristallografiya)* **1982**, *26*, 683.
(38) Parthé, E.; Chabot, B.; Hovestreydt, E. *Acta Crystallogr., Sect. B: Struct. Sci.* **1983**, *39*, 596.
(39) Pivan, J.-Y.; Guérin, R.; Sergent, M. *J. Solid State Chem.* **1987**, *68*, 11.
(40) Pivan, J.-Y.; Guérin, R.; Padiou, J.; Sergent, M. *J. Less-Common Met.* **1986**, *118*, 191.
(41) Asbrand, M.; Eisenmann, B. *Z. Anorg. Allg. Chem.* **1994**, *620*, 1837.

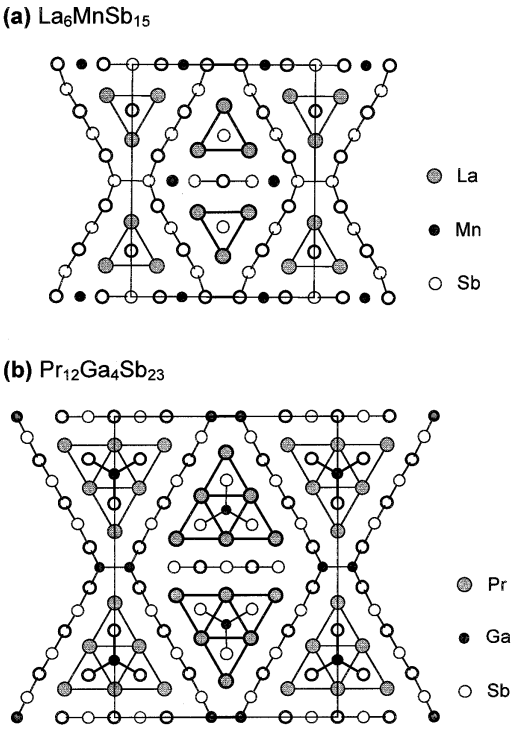

Figure 10. Comparison of the orthorhombic structures of (a) La_6MnSb_{15} and (b) $Pr_{12}Ga_4Sb_{23}$ shown in projection down the shortest axis. Circles with thicker rims are atoms residing in planes displaced by $^1/_2$ the short axis parameter.

at 50% occupancy at sites at the edge of the isolated Sb strip, but in $Pr_{12}Ga_4Sb_{23}$, these sites remain essentially vacant (2.7-(2)% Ga). In the same manner in which the hexagonal metal-rich structures such as $Ho_6Ni_{20}P_{13}$ can be regarded as belonging to a homologous series with increasingly larger triangular assemblies of trigonal prisms,[40] it is evident that La_6MnSb_{15} and $Pr_{12}Ga_4Sb_{23}$ form the first two members of a series of pseudohexagonal orthorhombic metalloid-rich structures, with the general formula $(RE)_{(n+1)(n+2)}(A)_{n(n-1)+2}(Sb)_{n(n+7)+5}$. Neglecting the partially occupied Mn site and recognizing that an Sb_2-pair in La_6MnSb_{15} takes the place of the Ga_2-pair in $Pr_{12}Ga_4Sb_{23}$, we can rewrite the formula of the $n = 1$ member as $RE_6A_2Sb_{13}$, where A = Sb. The $n = 2$ member is $RE_{12}A_4Sb_{23}$, exemplified by $Pr_{12}Ga_4Sb_{23}$. It would seem worthwhile, then, to attempt the syntheses of "$RE_6Ga_2Sb_{13}$" ($n = 1$) or "$RE_{20}Ga_8Sb_{35}$" ($n = 3$), although the small increments in the stoichiometric ratios and similar predicted X-ray diffraction patterns will make this a challenging task. Equally worthwhile would be to attempt substitutions of Ga with another main-group element such as Al, Si, or Ge.

Acknowledgment. This work was supported by the Natural Sciences and Engineering Research Council of Canada and the University of Alberta. We thank Dr. Robert McDonald (Faculty Service Officer, X-ray Crystallography Laboratory) and Dr. Michael Ferguson for the X-ray data collection, Christina Barker (Department of Chemical and Materials Engineering) for assistance with the EDX analyses, and Erica J. Anderson for assistance with the powder X-ray analyses.

Supporting Information Available: Listings of powder X-ray diffraction data for $RE_{12}Ga_4Sb_{23}$ (RE = La−Nd, Sm), further crystallographic details, and X-ray crystallographic files in CIF format. This material is available free of charge via the Internet at http://pubs.acs.org.

IC000519W